

# Determination of Key Cohesive Zone Model's Parameters for Orthotropic Paper and Its Static Fracture Simulation

WANG Yue, WANG Yongjian\*, LI Lingquan

College of Engineering, Nanjing Agricultural University, Nanjing 210031, P. R. China

(Received 18 December 2020; revised 19 January 2021; accepted 22 January 2021)

**Abstract:** Investigation of paper cutting process is vital for the design of cutting tools, but the fracture mechanism of paper cutting is still unclear. Here, we focus on the cutting process of paper, including the key parameters of cohesive zone model (CZM) for the orthotropic paper, to simulate the shear fracture process. Firstly, the material constants of the orthotropic paper are determined by longitudinal and transverse tensile test. Secondly, based on the tensile stress-strain curves, combined with damage theory and numerical simulations, the key parameters of the CZM for the orthotropic paper are obtained. Finally, a model III fracture is simulated to verify the accuracy of the model. Results show that the load-displacement curves obtained by the simulation is consistent with the test results.

**Key words:** orthotropic; cohesive zone model (CZM); paper; static fracture

**CLC number:** O346.1      **Document code:** A      **Article ID:** 1005-1120(2021)01-0117-07

## 0 Introduction

The rapid development of logistics industry has a high requirement on the characteristics of packaging paper in terms of tear resistance, tensile resistance and resistance to external shock load. Therefore, a variety of mechanical theories on paper, such as damage mechanics<sup>[1-2]</sup> and fracture mechanics<sup>[3-4]</sup> were proposed. Paper needs suitable cutting tools and cutting process to make sure the smoothness of the paper's edge for various products. However, cutting technology aimed at ensuring the edges of paper are smooth mostly depend on a large number of experiments, which means the fracture mechanism of paper is still unclear.

The mechanical properties of the paper have been studied for decades. He and Zhang<sup>[5]</sup> applied the nonlinear theory of thin plate to simulate the viscoelastic mechanical behavior of printing paper and obtained incremental equilibrium equation. Xie<sup>[6]</sup> reported a relationship between the shear modulus and elastic modulus, under the assumption of orthotropic paper. Based on the updated Lagrangian de-

scription, Ma et al.<sup>[7]</sup> derived the incremental equilibrium equations of triangular plate-shell elements for a geometrically nonlinear problem. He and Liu<sup>[8]</sup> obtained the integral form of stress and strain constitutive equation of the  $z$ -direction mechanistic model for printing paper by using Laplace transform. Additionally, the Nomex paper<sup>[9]</sup> and the honeycomb paper<sup>[10]</sup> were also studied, to make sure that the used packaging paper is strong enough. It is crucial to focus on paper's fracture deeply including mechanical properties of paper.

Many types of research on fracture mechanics of metal materials can be found, but only a few on paper. In the field of crack propagation, the cohesive zone model (CZM)<sup>[11-12]</sup> has been widely used in metal materials<sup>[13]</sup> and some other smart materials<sup>[14]</sup>. It is believed that the maximum traction and the critical fracture energy are the key parameters for CZM<sup>[15-16]</sup>. In most literatures, these two key parameters were obtained by specific experiments<sup>[17]</sup> or numerical simulations<sup>[18]</sup>, both of which are complicated and expensive. Hence, Wang and Ru<sup>[19]</sup>

\*Corresponding author, E-mail address: yjwang@njau.edu.cn.

**How to cite this article:** WANG Yue, WANG Yongjian, LI Lingquan. Determination of key cohesive zone model's parameters for orthotropic paper and its static fracture simulation[J]. Transactions of Nanjing University of Aeronautics and Astronautics, 2021, 38(1):117-123.

<http://dx.doi.org/10.16356/j.1005-1120.2021.01.011>

proposed a new method to determine the two key parameters for X80 pipeline steel, based on the damage mechanics and numerical simulations. Shi and Wang<sup>[20]</sup> studied the shape of the traction-separation law (TSL) of the CZM, and found that the shape of TSL does not affect the global response for the quasi-static fracture. However, to the best of the author's knowledge, it is not reported that the two key parameters were obtained without specific experiments and numerical simulations for the paper fracture. To cover this gap, the current study proposed an engineering method to determine the two key CZM parameters for an orthotropic paper, which can help some related researchers to obtain the best cutting process parameters and the best size of cutting tools to make sure the smoothness of the paper's edge.

## 1 Mathematical Model

To be simplified, it is assumed to be orthotropic in the proposed model<sup>[6]</sup>, and its constitutive equation is as follows<sup>[21]</sup>

$$\begin{bmatrix} \sigma_{11} \\ \sigma_{22} \\ \sigma_{33} \\ \sigma_{23} \\ \sigma_{31} \\ \sigma_{12} \end{bmatrix} = \begin{bmatrix} c_{11} & c_{12} & c_{13} & 0 & 0 & 0 \\ c_{12} & c_{22} & c_{23} & 0 & 0 & 0 \\ c_{13} & c_{23} & c_{33} & 0 & 0 & 0 \\ 0 & 0 & 0 & c_{44} & 0 & 0 \\ 0 & 0 & 0 & 0 & c_{55} & 0 \\ 0 & 0 & 0 & 0 & 0 & c_{66} \end{bmatrix} \begin{bmatrix} \epsilon_{11} \\ \epsilon_{22} \\ \epsilon_{33} \\ \epsilon_{23} \\ \epsilon_{31} \\ \epsilon_{12} \end{bmatrix} \quad (1)$$

where  $\sigma_{ij}$ ,  $\epsilon_{ij}$  and  $c_{ij}$  are the stress, the strain and the stiffness matrix coefficients. The stiffness matrix  $C$  has the following relationship with the elastic modulus and Poisson's ratio<sup>[21]</sup>.

$$C^{-1} = \begin{bmatrix} \frac{1}{E_1} & -\frac{\nu_{12}}{E_2} & -\frac{\nu_{13}}{E_3} & 0 & 0 & 0 \\ -\frac{\nu_{21}}{E_1} & \frac{1}{E_2} & -\frac{\nu_{23}}{E_3} & 0 & 0 & 0 \\ -\frac{\nu_{31}}{E_1} & -\frac{\nu_{32}}{E_2} & \frac{1}{E_3} & 0 & 0 & 0 \\ 0 & 0 & 0 & \frac{1}{G_{23}} & 0 & 0 \\ 0 & 0 & 0 & 0 & \frac{1}{G_{31}} & 0 \\ 0 & 0 & 0 & 0 & 0 & \frac{1}{G_{12}} \end{bmatrix} \quad (2)$$

where,  $E_i$  is the elastic modulus along the  $i$  direction, and  $\nu_{ij}$  and  $G_{ij}$  are the Poisson's ratio and shear modulus, respectively. Due to the symmetry of the stiffness matrix, there are<sup>[21]</sup>

$$\begin{aligned} \frac{\nu_{12}}{E_2} &= \frac{\nu_{21}}{E_1} \\ \frac{\nu_{23}}{E_3} &= \frac{\nu_{32}}{E_2} \\ \frac{\nu_{13}}{E_3} &= \frac{\nu_{31}}{E_1} \end{aligned} \quad (3)$$

The tensile test samples were performed along with the longitudinal and transverse directions. The size of tensile test sample is shown in Fig.1, and the thickness of the paper is 0.4 mm. The wider area of 70 mm×20 mm on both sides is the grip section, the area of 80 mm×13 mm in the middle is the effective section of the experiment, the rounded corner of 15 mm is the transition zone.

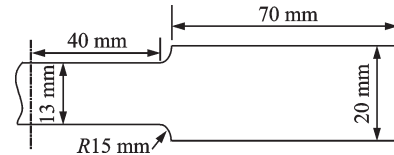


Fig.1 Size of tensile test sample (half sample)

The stress-strain curves are obtained by five tensile tests on transverse and longitudinal directions, as shown in Fig.2. After taking the average value (thick line in Fig.2), the transverse and longitudinal elastic modulus can be obtained as  $E_1 = 1065.8$  MPa and  $E_2 = 563.22$  MPa.

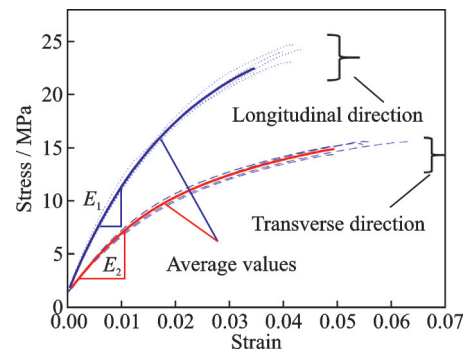


Fig.2 Stress-strain curves for transverse and longitudinal directions

The relationship between shear modulus and elastic modulus is given by Xie<sup>[6]</sup>

$$\begin{aligned}
 G_{12} &= \frac{E_1 E_2}{E_1 + E_2 (1 + 2\nu_{12})} \\
 G_{23} &= \frac{E_2 E_3}{E_2 + E_3 (1 + 2\nu_{23})} \\
 G_{31} &= \frac{E_3 E_1}{E_3 + E_1 (1 + 2\nu_{31})}
 \end{aligned} \quad (4)$$

Let  $\nu_{12} = 0.34^{[6]}$ , and thus  $G_{12} = 298.35$  MPa.

A micro indentation instrument was used to find  $E_3$  along the thickness direction, the needle size is  $50 \mu\text{m} \times 50 \mu\text{m}$ . The stress-strain curves along the thickness for both sides of the paper were shown in Fig. 3. After taking the average of the curves (thick line in Fig. 3), the elastic modulus of the rough and smooth surface were obtained:  $E_{3c} = 278.15$  MPa,  $E_{3s} = 392.79$  MPa, and thus the average value is  $E_3 = 335.47$  MPa.

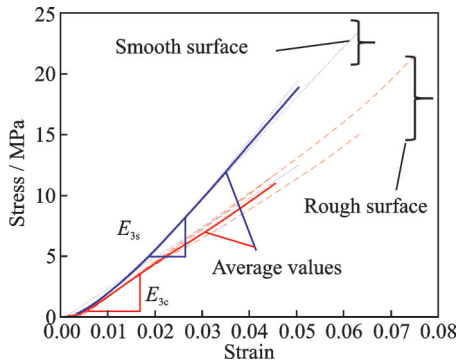


Fig.3 Stress-strain curves along the thickness direction of smooth and rough surfaces

Let  $\nu_{23} = \nu_{31} = 0.01^{[6]}$ , and thus according to Eq. (4),  $G_{23} = 208.69$  MPa,  $G_{31} = 251.33$  MPa. The engineering material constants are listed in Table 1. Substituting the engineering material constants into Eq.(2), the stiffness matrix can be obtained.

**Table 1 Engineering material constants**

Elastic modulus	Value/MPa	Poisson's ratio	Value	Shear modulus	Value/MPa
$E_1$	1 065.80	$\nu_{12}$	0.34 <sup>[6]</sup>	$G_{12}$	298.35
$E_2$	563.22	$\nu_{23}$	0.01 <sup>[6]</sup>	$G_{23}$	208.69
$E_3$	335.47	$\nu_{31}$	0.01 <sup>[6]</sup>	$G_{31}$	251.33

## 2 Analysis of Parameters

A bilinear TSL was chosen in this paper, subsequently the shape of the TSL of CZM has limited

influence on the macro response of the structure<sup>[20]</sup>, as shown in Fig.4.  $T_{\max}$  is the maximum traction,  $S_0$  the corresponding separation where the damage was beginning, and  $S_{\max}$  the maximum separation at the fracture point. The area enclosed to the TSL curve is the critical fracture energy, denoted as  $J$ , and the maximum traction  $T_{\max}$  and the critical fracture energy  $J$  are the two key parameters for CZM.

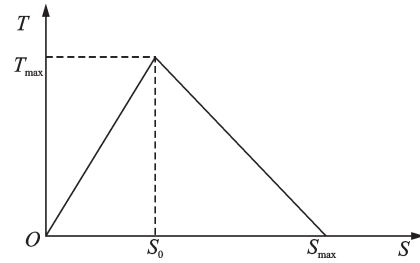


Fig.4 Bilinear TSL for a CZM

### 2.1 Critical fracture energy

Based on the material constants obtained by transverse and longitudinal tensile tests, the critical fracture energy will be estimated by numerical simulations<sup>[19]</sup>.

A two-dimensional tensile specimen model<sup>[19]</sup> is established, as shown in Fig.1. The left end was fixed and the right end was loaded at a speed of 3 mm/s. To obtain the value of J-integral, the crack tip is arranged in the middle of the specimen, with a length of 0.1 mm. There are 744 CPS8R elements in this model, and the mesh at the crack tip is shown in Fig.5.

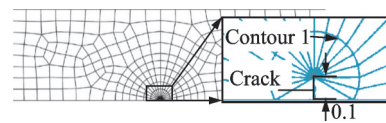


Fig.5 Half model of a model I crack specimen

The relationship between J-integral, nominal strain and analysis step time are shown in Fig. 6. When the global nominal strain given by the universal testing machine reaches the fracture strain, the corresponding J-integral value achieves as critical fracture energy. It can be seen in Fig.6, the critical fracture energies for longitudinal and transverse directions are  $120.8 \text{ J/m}^2$  and  $104.8 \text{ J/m}^2$ , respectively.

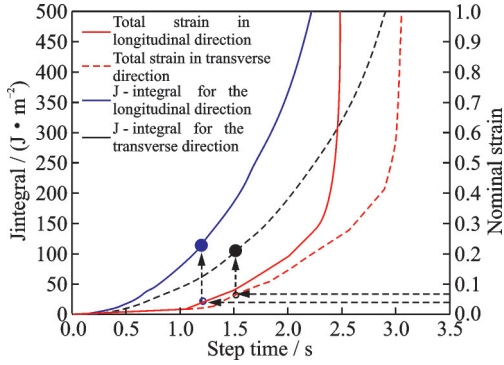


Fig.6 Critical fracture energies for transverse and longitudinal directions (Model I crack)

To obtain the critical fracture energy for model III crack, a three-dimensional model with a thickness of 0.4 mm and a notch of 90° at the crack tip is established, as shown in Fig.7. The left side with 5 mm under the crack is fixed but the other side is loaded at a speed of 3 mm/s. A total of 1 872 C3D20 elements were used in this model. The same as the tensile test simulation, the corresponding J-integral value is the critical fracture energy as the total strain reaches the fracture strain.

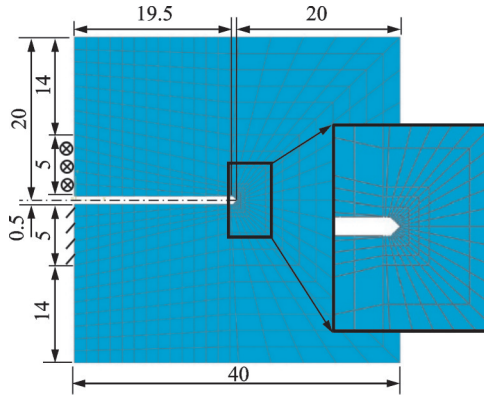


Fig.7 Sizes and boundary conditions of the model III crack (Unit:mm)

In Fig. 8, the critical fracture energies of model III crack for longitudinal and transverse directions are 28.47 J/m<sup>2</sup> and 27.27 J/m<sup>2</sup>.

## 2.2 Maximum traction

According to the tensile test, the critical fracture stresses here are  $\sigma_{\max}^1 = 24.68$  MPa and  $\sigma_{\max}^2 = 15.58$  MPa. Based on the principle of damage mechanics, a damage factor  $d$  is introduced, and the

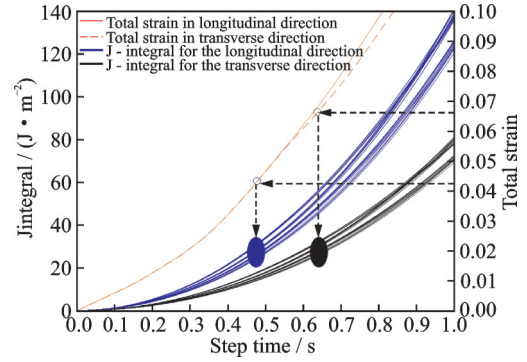


Fig.8 Critical fracture energies for transverse and longitudinal directions (Model III crack)

critical stress is the maximum traction, which can be expressed as<sup>[19]</sup>

$$\sigma_c = T_{\max} = \frac{\sigma_{\max}}{1-d} \quad (5)$$

Let  $d = 0.3$ , and the maximum tractions for the CZM are  $T_{\max}^{11} = 35.26$  MPa and  $T_{\max}^{22} = 22.25$  MPa.

According to the simulation results of the model III crack, the critical shear strain corresponding to the total strain at the crack tip for transverse and longitudinal directions are  $\epsilon_{\max}^{32} = 0.044$  and  $\epsilon_{\max}^{31} = 0.068$ . Thus, the corresponding shear stress are  $\sigma_{\max}^{32} = 1.58$  MPa and  $\sigma_{\max}^{31} = 2.42$  MPa. Substituted these values into Eq. (5), the maximum tractions for model III crack can be obtained, i.e.,  $T_{\max}^{32} = 2.26$  MPa and  $T_{\max}^{31} = 3.45$  MPa.

Above all, the key parameters of CZM for models I and III cracks on the orthotropic paper are shown in Table 2. It can be seen that the maximum traction and fracture energy for the model III crack are much smaller than that of the model I crack, which is consistent with the existing literature findings.

## 3 Discussion

To verify CZM, the fracture of the model III crack is simulated. Fig.9 shows the size of the specimen, with a thickness of 0.4 mm. The cohesive surface (red line in Fig.9) is used to represent the direction of crack propagation. There are a total of 36 000 C3D8R and 61 506 C3D6 elements. The left

**Table 2 Key parameters of CZM for model I and model III cracks**

Crack type	Maximum traction / MPa	Critical fracture energy / ( $\text{J}\cdot\text{m}^{-2}$ )	$S_0$ / m
Model I	$T_{\max}^{11} = 35.26$	120.8	$S_0 = 2 \times 10^{-6}$
	$T_{\max}^{22} = 22.25$	104.8	
Model III	$T_{\max}^{31} = 3.45$	28.47	
	$T_{\max}^{32} = 2.26$	27.27	

10 mm length of the notch is fixed, and the right 10 mm length of the notch is loaded at a speed of 10 mm/min.

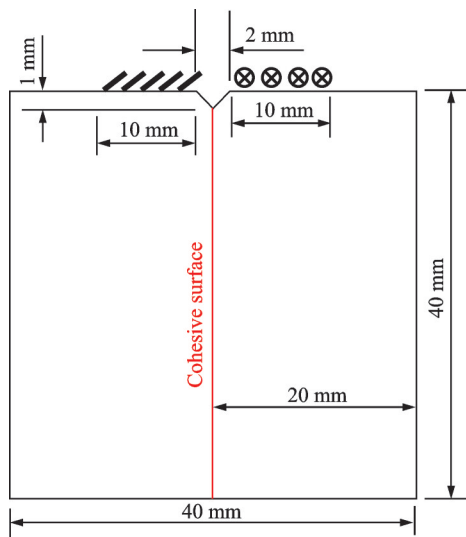


Fig.9 Simulation of the fracture for model III crack

Fig. 10 shows the load-displacement curves for the simulation and experimental results. It can be seen that the simulation results agreed well with the experimental results for both longitudinal and transverse directions. Once the load begins to drop, the paper has been torn. For the experiments, it is difficult to make sure that the mode III crack propagates along the planned route. Furthermore, in most cases, the layers of paper will be pulled apart after the load decreased. However, the simulation test does not consider the interaction between layers of paper. Therefore, only the beginning of the model III fracture was compared.

## 4 Conclusions

During the paper cutting process, burr along the cutting side are mostly not considered. The main

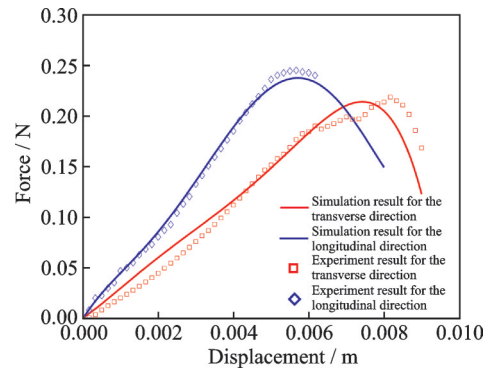


Fig.10 Comparison of load-displacement curves between results of simulations and experiments

reason is that the mechanical behavior of paper cutting is unclear. In this paper, the model III fracture based on CZM for the orthotropic paper was studied. The material constants for the orthotropic paper were obtained by tensile and micro indentation tests. Based on the tensile test, the maximum traction and the critical fracture energy of CZM were obtained according to the damage mechanics and numerical simulations. The model III fracture of the orthotropic paper was simulated to verify the accuracy of CZM. By comparing the load displacement curves between the results of simulations and experiments, it is proved that the key CZM parameters estimated in this paper are reasonable and credible.

## References

- [1] ISAKSSON P, GRADIN P A, KULACHENKO A. The onset and progression of damage in isotropic paper sheets[J]. International Journal of Solids and Structures, 2006(43): 713-726.
- [2] ISAKSSON P, HEAGGLUND R, GRADIN P. Continuum damage mechanics applied to paper[J]. International Journal of Solids and Structures, 2004 (41): 4731-4755.
- [3] YUHARA T, KORTSCHOT M T. A simplified determination of the J-integral for paper[J]. Journal of

- Materials Science, 1993(28): 3571-3580.
- [4] DING Qijun, ZENG Jinsong, WANG Bin, et al. Effect of retention rate of fluorescent cellulose nanofibrils on paper properties and structure[J]. Carbohydrate Polymers, 2018(186): 73-81.
- [5] HE Zifen, ZHANG Yinhui. Study of the mechanical properties of printable paper based on nonlinear finite element method[J]. Packaging Engineering, 2008(4): 54-56. (in Chinese)
- [6] XIE Yihuan. Relationship between elastic modulus and shear modulus of paper[J]. Packaging Engineering, 2012, 33(21): 37-40. (in Chinese)
- [7] MA Junxing, YANG Shenjun, HE Zhengjia, et al. Mechanical properties of office paper analyzed by using nonlinear finite element method[J]. Journal of Xi'an Jiaotong University, 2000, 34(9): 67-71. (in Chinese)
- [8] HE Zifen, LIU Xin. Study on Z-direction mechanical properties of printing paper[J]. Packaging Engineering, 2004, 25(6): 24-25, 46. (in Chinese)
- [9] WANG Houlin, WANG Yi, YAO Yunzhen, et al. The relationship between aramid paper honeycomb mechanical properties and paper performance[J]. Journal of Functional Materials, 2013, 44(3): 349-352. (in Chinese)
- [10] PENG Jianlin. Study on mechanical properties of honeycomb paperboard[D]. Kunming: Kunming University of Science and Technology, 2008.
- [11] Dugdale D. Yielding of steel sheets containing slits[J]. Journal of the Mechanics and Physics of Solids, 1960, 8(2): 100-104.
- [12] BARENBLATT G I. The mathematical theory of equilibrium cracks in brittle fracture[J]. Advances in Applied Mechanics, 1962, 7: 622-636.
- [13] REN Zhongjun, RU Chongqin. Numerical investigation of speed dependent dynamic fracture toughness of line pipe steels[J]. Engineering Fracture Mechanics, 2013(99): 214-222.
- [14] UTZINGER J, STEINMANN P, MENZEL A. On the simulation of cohesive fatigue effects in grain boundaries of a piezoelectric mesostructured[J]. International Journal of Solids and Structures, 2008, 45(17): 4687-4708.
- [15] ELICES M, GUINEA G, GOMEZ J, et al. The cohesive zone model: Advantages, limitations and challenges[J]. Engineering Fracture Mechanics, 2002, 69(2): 137-163.
- [16] CORNEC A, SCHEIDER I, SCHWALBE K H. On the practical application of the cohesive model[J]. Engineering Fracture Mechanics, 2003, 70(14): 1963-1987.
- [17] SONG S H, PAULINO G H, BUTTLAR W G. Simulation of crack propagation in asphalt concrete using an intrinsic cohesive zone model[J]. Journal of Engineering Mechanics, 2006, 132(11): 1215-1223.
- [18] YU Peishi, RU Chongqin. Strain rate effects on dynamic fracture of pipeline steels: Finite element simulation[J]. International Journal of Pressure Vessels and Piping, 2015(126/127): 1-7.
- [19] WANG Yongjian, RU Chongqin. Determination of two key parameters of a cohesive zone model for pipeline steels based on uniaxial stress-strain curve[J]. Engineering Fracture Mechanics, 2016(163): 55-65.
- [20] SHI Yan, WANG Yongjian. Shape effects of the traction - separation law on the global response of the dynamic fracture for pipeline steels[J]. Acta Mechanica, 2019(230): 1403-1412.
- [21] FEI Kang. Application of ABAQUS in geotechnical engineering [M]. Beijing: China Water & Power Press, 2010: 62-64.

**Acknowledgement** This work was supported by the National Natural Science Foundation of China (No. 11702147).

**Authors** Mr. WANG Yue received the B. S. degree in mechanical engineering from ZiJin College Nanjing University of Science and Technology, Nanjing, China, in 2019. He is currently a postgraduate at Nanjing Agricultural University.

Dr. WANG Yongjian received the Ph.D. degree in solid mechanics from Nanjing University of Aeronautics and Astronautics, Nanjing, China, in 2012. From 2014 to 2015, he was a Postdoctoral Research Fellow in the department of Mechanical Engineering, University of Alberta, Alberta, Canada. From 2012 to present, he has been with the College of Engineering, Nanjing Agricultural University, where he is currently a full associate professor. His research has focused on the dynamic fracture mechanics for different materials, including metal, piezoelectric materials, soil, and crop's straw.

**Author contributions** Dr. WANG Yongjian designed the study and wrote the manuscript. Mr. WANG Yue contributed data for the simulation part. Mr. LI Lingquan

contributed data for the experiment part. All authors commented on the manuscript draft and approved the submission.

**Competing interests** The authors declare no competing interests

(Production Editor: ZHANG Tong)

## 正交各向异性纸张内聚区模型关键参数的确定 及其静态断裂仿真

王 越, 王永健, 李令全

(南京农业大学工学院, 南京 210031, 中国)

**摘要:** 研究纸张裁剪过程对刀具设计至关重要, 然而纸张裁剪的断裂机理却尚未明晰。为此, 基于内聚区模型, 对纸张的剪切过程进行仿真分析, 并给出确定纸张剪切内聚区模型关键参数的方法。首先, 通过纸张的纵向和横向拉伸试验, 基于各向异性理论, 确定纸张的材料常数。其次, 基于拉伸应力-应变曲线, 结合损伤理论和数值方法, 给出纸张内聚区模型的关键参数: 最大张力和内聚能。最后, 对纸张的剪切试验进行仿真模拟, 以验证模型的准确性。结果表明: 静态断裂下, 剪切试验的全局载荷-位移曲线与试验结果基本一致, 验证了模型的可靠性。

**关键词:** 正交各向异性; 内聚区模型; 纸张; 静态断裂